SLAC-PUB-4275
LBL-22691
April 1987
(M)

OBSERVATION OF A SPIN 1 RESONANCE IN THE REACTION $\gamma\gamma^* \to K^0 K^\pm \pi^\mp$[†]

G. Gidal, J. Boyer, F. Butler, D. Cords, G.S. Abrams, D. Amidei[a], A.R. Baden, T. Barklow, A.M. Boyarski, P. Burchat[b], D.L. Burke, J.M. Dorfan, G.J. Feldman, L. Gladney[c], M.S. Gold, G. Goldhaber, L.J. Golding[d], J. Haggerty[e], G. Hanson, K. Hayes, D. Herrup, R.J. Hollebeek[c], W.R. Innes, J.A. Jaros, I. Juricic, J.A. Kadyk, D. Karlen, S.R. Klein, A.J. Lankford, R.R. Larsen, B.W. LeClaire, M.E. Levi, N.S. Lockyer[c], V. Lüth, C. Matteuzzi[f], M.E. Nelson[g], R.A. Ong, M.L. Perl, B. Richter, K. Riles, P.C. Rowson[h], T. Schaad[i], H. Schellman[a], W.B. Schmidke, P.D. Sheldon[j], G.H. Trilling, C. de la Vaissière[k], D.R. Wood, J.M. Yelton[l], and C. Zaiser

Lawrence Berkeley Laboratory and Department of Physics
University of California, Berkeley, California 94720

Stanford Linear Accelerator Center
Stanford University, Stanford, California 94305

Department of Physics
Harvard University, Cambridge, Massachusetts 02138

Abstract

We confirm the observation of a spin 1 resonance at 1423 MeV in the $K_S^0 K^\pm \pi^\mp$ system produced in single tagged two photon interactions. The Dalitz plot indicates that this resonance decays primarily via a K^*K intermediate state. We measure a radiative width times branching ratio $B_{K\overline{K}\pi} \cdot \frac{M^2}{Q^2} \cdot \Gamma_{\gamma\gamma^*} = 2.7 \pm 1.2 \pm 0.5$ keV assuming a ρ-pole form factor.

Submitted for Publication

[†]This work was supported in part by the Department of Energy under contracts DE-AC03-76SF00098, DE-AC03-76SF00515, and DE-AC02-76ER03064.

[a]Present address: University of Chicago, Chicago, IL 60637

[b]Present address: University of California, Santa Cruz, CA 95064

[c]Present address: University of Pennsylvania, Philadelphia, PA 19104

[d]Present address: Therma-Wave Corporation, Fremont, CA 94539

[e]Present address: Brookhaven National Laboratory, Upton, NY 11973

[f]Present address: CERN, CH-1211 Geneva 23, Switzerland

[g]Present address: California Institute of Technology, Pasadena, CA 91125

[h]Present address: Columbia University, New York, NY 10027

[i]Present address: University of Geneva, CH-1211 Geneva 4, Switzerland

[j]Present address: University of Illinois, Urbana, IL 61801

[k]Present address: LPNHE, Univ. Pierre Marie Curie, Paris, France F-75230

[l]Present address: Oxford University, Oxford, England

Two mesons, the $\eta(1440)$ and $f_1(1420)$ appear at nearly the same mass in a wide variety of experiments. Different experiments obtain different spin parity assignments for mesons in this mass region, although most radiative J/ψ decay experiments obtain $J^P = 0^-$ and a mass near 1450 MeV,[1] while hadroproduction experiments find $J^P = 1^+$ or 0^- and a mass near 1420 MeV.[2]

The $K^0K^\pm\pi^\mp$ final state is a major decay mode of the $\eta(1440)$ and $f_1(1420)$ and so can be used to study their production in photon-photon interactions. Although rather stringent limits[3] have been placed on $\Gamma(\eta(1440) \to \gamma\gamma)$ where the photons are on mass shell, the PEP 4/9 group has recently reported[4] evidence for a state near 1420 MeV in the $K^0K^\pm\pi^\mp$ system produced in tagged $\gamma\gamma^*$ interactions. We report on a similar study with 220 pb^{-1} of data taken with the Mark II detector at PEP and confirm this observation.[5] The production at only larger Q^2, indications of a dominant K^*K decay mode, and our failure to observe it in $\eta\pi^+\pi^-$, lead us to tentatively identify this state with the $J^{PC} = 1^{++} f_1(1420)$.

The major features of the Mark II detector have been well described elsewhere.[6] Charged tracks are measured in the central drift chamber and the vertex drift chamber, with a precision $\Delta p/p = [(0.025)^2 + (0.01p(\mathrm{GeV}))^2]^{\frac{1}{2}}$. The position and energy of the photons are measured in eight liquid argon barrel calorimeter modules with an energy resolution of $0.14/\sqrt{E(\mathrm{GeV})}$. The Pb-proportional chamber endcap calorimeters are primarily used to veto events with extra photons. The 2.3 kG solenoidal magnetic field

allows low p_T pions to reach the TOF counters and hence trigger the detector. The small angle tagging system and shower counter (SAT) identify and measure scattered electrons at polar angles between 21 and 83 mrad from the incident e^+ or e^- direction. Events with one SAT track having energy greater than 7 GeV are accepted in this analysis. To study the reaction

$$e^+e^- \rightarrow e^+e^-K^0K^\pm\pi^\mp \tag{1}$$

we further select events with four charged tracks of net charge zero in the central detector. We then require that two of these tracks reconstruct to a K^0_S which decays at least 2.0 mm from the primary vertex. The projection of these two tracks to the secondary vertex, cuts that require a positive flight path and $480 < m_{\pi^+\pi^-} < 520$ MeV, defines the K^0_S sample. The distribution in $m_{\pi^+\pi^-}$ before the last cut is shown in Figure 1 and indicates very little background. To eliminate a possible $f'(1520) \rightarrow K^0_S\overline{K}^0_S$ background we remove events in which the $\pi^+\pi^-$ pair opposite the identified K^0_S has an invariant mass between 480 and 520 MeV. Most tracks produced by reaction (1) have momenta below 1 GeV/c and therefore, whenever possible, time of flight information is used to identify the charged K and π tracks. Each candidate event is then examined in detail for such things as untracked $K^\pm$ decays, poorly measured tracks, and especially for extra gammas detected in the liquid argon barrel calorimeters or the proportional chamber endcaps, that are not associated with charged tracks. The events with extra gammas are primarily feeddown from higher multiplicity $\gamma\gamma^*$ interactions and form a sample that can be used to study potential backgrounds to reaction (1).

The net transverse momentum with respect to the e^+e^- axis, Σp_T, including the measured outgoing beam electron or positron is required to be less than 150 MeV/c. There remain 27 events attributed to reaction (1). All but one of these have only one combination of tracks consistent with the $K^0K^\pm\pi^\mp$ hypothesis, and we plot their invariant masses in Figure 2a. Note the dominant peak between 1400 and 1500 MeV. A fit in 20 MeV bins to a gaussian distribution gives $m = 1423 \pm 4$ MeV and $\sigma = 14 \pm 2$ MeV, consistent with the detector resolution determined with Monte Carlo simulations. The invariant mass of the background events with extra gammas is shown in Figure 2b. These events show no peaking. Figure 2c shows the scatter plot of the invariant four momentum transfer Q^2 vs. $M(K^0K^\pm\pi^\mp)$. The peak events are clearly produced at relatively large Q^2 confirming the PEP 4/9 observations. The absence of such a peak in $\gamma\gamma$ interactions at $Q^2 \simeq 0$ has already been noted with sufficient sensitivity.[3] Since real photon-photon collisions cannot produce a spin 1 particle,[7] while a spin 0 particle would be produced even more copiously in such collisions, we assume this peak to be spin 1.

In Figure 3a we show the Dalitz plot for the 13 events with masses between 1.4 and 1.5 GeV. Although the statistics are limited, the events appear to be grouped in the $K^*(890)$ bands. The Dalitz plot for the sidebands ($1.3 < m < 1.4$ and $1.5 < m < 1.6$ GeV) together with the corresponding ($1.3 < m < 1.6$ GeV) background "extra photon" events is shown in Figure 3b and shows no clustering in the K^* bands. Alternatively, a decay via the $a_0(980)\pi$ intermediate state would have resulted in a clear signal in the $\eta^0\pi^+\pi^-$ final state, since the $a_0(980)$ decays predominantly into $\eta\pi$. No such signal was seen.[11]

To measure the detection efficiency we generate Monte Carlo events for a 1425 MeV spin 1 resonance, R, with helicity 1 and with an equal mixture of $K^{*0}K^0$ and $K^{*-}K^+$ decays. The same careful scanning procedure is applied to these Monte Carlo events, to obtain the final detection efficiency. The 11 events above background in Figure 2a then correspond to a cross section, $\sigma(e^+e^- \to e^+e^-R) = 10.3 \pm 4.0 \pm 1.5$ pb over the Q^2 interval 0.2–1.1 $(\mathrm{GeV}/c)^2$. Following Cahn[8] we parameterize this observed cross section as

$$\sigma_{e^+e^-\to e^+e^-R} = 15.1\tilde{\Gamma}\ (\mathrm{keV}) \left[\int \frac{dQ^2}{M^2} F^2(Q^2) + 0.53 \int \frac{dQ^2}{M^2} \cdot \frac{Q^2}{M^2} \cdot F^2(Q^2) \right] \cdot C(\tau)\ \mathrm{pb} \quad (2)$$

where $\tilde{\Gamma}_{R\gamma\gamma^*} = \left(\frac{M_R^2}{Q^2}\right) \Gamma_{R\gamma\gamma^*}$ in the low Q^2 limit, $\tau = \frac{M_R^2}{s}$ and the residual Q^2 dependence is contained in the form factor, for which we assume the form $F(Q^2) = \frac{1}{1+Q^2/m_\rho^2}$. The factor $C(\tau) = 0.96$ is the ratio of the exact $\gamma\gamma^*$ luminosity to that used in reference (8). From Equation (2) evaluated at $\sqrt{s} = 29$ GeV, $M_R = 1.425$ GeV and $m_\rho = 0.76$ GeV we obtain from our cross section measurement, over the Q^2 interval 0.2–1.1 $(\mathrm{GeV}/c)^2$, $B(R \to K\overline{K}\pi) \cdot \tilde{\Gamma}_{R\gamma\gamma^*} = 2.7 \pm 1.2 \pm 0.5$ keV, lower than the PEP 4/9 value[4] of $6 \pm 2 \pm 2$ keV. It is important to note that this result is sensitive to the assumed Q^2 dependence. For example, an $F(Q^2) = \frac{1}{1+Q^2/m_\phi^2}$, which might be more appropriate for a resonance with quark composition $s\bar{s}$, would yield a $BR(R \to K\overline{K}\pi)\tilde{\Gamma}(R \to \gamma\gamma^*) = 1.7 \pm 0.8 \pm 0.3$ keV.

The axial vector nonet is usually taken to consist of the $a_1(1270)$, $K_{1A}(1340)$, $f_1(1285)$ and $f_1(1420)$ with ideal mixing, i.e., with quark composition $f_1(1285) \sim (u\bar{u} + d\bar{d})/\sqrt{2}$ and $f_1(1420) \sim s\bar{s}$. However, a non-relativistic quark model with these assumptions predicts[9,10] that $\tilde{\Gamma}(f_1(1420) \to \gamma\gamma^*) = \frac{2}{15}\frac{M_{f_1}}{M_{f_2}}\Gamma(f_2(1270) \to \gamma\gamma) \cong 0.4$ keV, almost an

order of magnitude smaller than our measurement assuming $B(R \to K\overline{K}\pi) = 1$. The model also predicts that $\tilde{\Gamma}(f_1(1285) \to \gamma\gamma^*)/\tilde{\Gamma}(f_1(1420) \to \gamma\gamma^*) \cong \frac{25}{2}\frac{M_{f_1(1285)}}{M_{f_1(1420)}}$, again larger than our measured ratio[11] of 3.0 ± 1.6. A small deviation from ideal mixing can however accommodate these measurements.

Although the $f_1(1285)$ can also decay into $K\overline{K}\pi$, no significant signal is seen at this mass in Figure 2a. From the 3 events below 1.35 GeV we can calculate a limit $B(f_1(1285) \to K\overline{K}\pi)\tilde{\Gamma}(f_1(1285) \to \gamma\gamma^*) < 0.92$ keV (95% C.L.). Our previous measurement[11] of $\tilde{\Gamma}(f_1(1285) \to \gamma\gamma^*) = 8.2 \pm 1.8 \pm 0.9$ keV and a branching ratio[12] to $K\overline{K}\pi$ of 0.11 ± 0.03 are consistent with this limit.

Based on the relatively large $f_1(1420)$ radiative width and recent observations in hadronic J/ψ decays, Chanowitz[10] has suggested that the observed state is a candidate for an exotic $J^{PC} = 1^{-+}$ hybrid $q\bar{q}g$ state (or meikton). A direct test of the spin-parity is obtained from the folded distribution in the cosine of the angle θ between the normal to the decay plane and the incident photon, in the rest frame of the $f_1(1420)$. Cahn[8] has pointed out that at small Q^2 the distribution is $1 + \cos^2\theta$ for a $J^{PC} = 1^{++}$ particle and is $1 - \cos^2\theta$ for a $J^{PC} = 1^{-+}$ particle. Figure 4 shows the resultant measured folded distribution, normalized to the Monte Carlo simulation, for the 13 events between 1.400 and 1.500 GeV, together with the expectations[13] from those predictions. No definite conclusion is possible for so few events.

In summary, we have observed a peak near 1425 MeV in $\gamma\gamma^* \to K^0K^\pm\pi^\mp$ with a Q^2 distribution characteristic of a spin 1 resonance. We tentatively identify it with the

$J^{PC} = 1^{++} f_1(1420)$, although a departure from ideal mixing is required to accommodate the measured $f_1(1285)$ and $f_1(1420)$ radiative widths in the naive quark model. A more definitive identification awaits a higher statistics spin-parity determination.

We gratefully acknowledge helpful discussions with R. Cahn and M. Chanowitz.

References

1. C. Edwards et al., Phys. Rev. Lett. 49 (1982) 259; D. Hitlin, Aspen Winter Conf., Jan. 12-18, 1986.

2. C. Dionisi et al., Nucl. Phys. *B*169 (1980) 1; T.A. Armstrong et al., Phys. Lett. 146*B* (1984) 273; D. Aston et al., Phys. Rev. *D*32 (1985) 2255; S.U. Chung et al., Phys. Rev. Lett. 55 (1985) 779; A. Ando et al., Phys. Rev. Lett. 57 (1986) 1296.

3. H. Aihara et al., Phys. Rev. Lett. 57 (1986) 51; G. Gidal, in Multiparticle Dynamics, 1985 (World Scientific).

4. J.C. Sens et al., Contribution to VIIth International Workshop on Photon-Photon Collisions, College de France, Paris, April 1-5, 1986; H. Aihara et al., Phys. Rev. Lett. 57, 2500 (1986).

5. A preliminary report of these results was presented at the 23rd International Conference on High Energy Physics, Berkeley, California, July 16-23, 1986 (World Scientific).

6. R.H. Schindler et al., Phys. Rev. *D*24 (1981) 78; G.S. Abrams et al., IEEE Trans. Nucl. Sci. 27 (1980) 59.

7. C.N. Yang, Phys. Rev. 77 (1950) 242; L.F. Landau, Dokl. Akad. Nauk. SSSR 60 (1948) 207.

8. R.N. Cahn, Production of Spin-One Resonances in $\gamma\gamma^*$ Collisions, LBL-22555, December 1986 (submitted to Phys. Rev. D.). For small luminosity corrections see J.H. Field, Nucl. Phys. *B*168 (1980) 477; Erratum, Nucl. Phys. *B*176 (1980) 545.

9. F.M. Renard, Nuovo Cimento 80*A* (1984) 1.

10. M.S. Chanowitz, An Exotic Quark-Gluon Hybrid at 1420 MeV?, LBL-22611, December 1986.

11. G. Gidal et al., LBL-22690 (submitted to Phys. Rev. Lett.).

12. Review of Particle Properties, Phys. Lett. 170*B* (1986) 1. Throughout this paper we use the established meson notation.

13. The expected angular distributions have been corrected for the finite Q^2 interval sampled, to order Q^2/M^2 (J. Boyer and R.N. Cahn, private communication).

Figure Captions

Fig. 1. Invariant mass of $\pi^+\pi^-$ pairs used to define the K_S^0 sample.

Fig. 2. The $K_S^0 K^\pm \pi^\mp$ invariant mass for (a) the accepted event sample and (b) the events with extra gammas. The scatter plot (c) shows this invariant mass vs. Q^2 for the accepted events.

Fig. 3. The Dalitz plot for (a) accepted events and (b) background sample.

Fig. 4. The measured distribution in $|\cos\theta|$ for the events with $1.4 < m(K_s^0 K^\pm \pi^\mp) < 1.5$ GeV. The solid (dashed) histograms are the result of Monte Carlo simulations of the distributions expected for $J^{PC} = 1^{++}$ ($J^{PC} = 1^{-+}$).

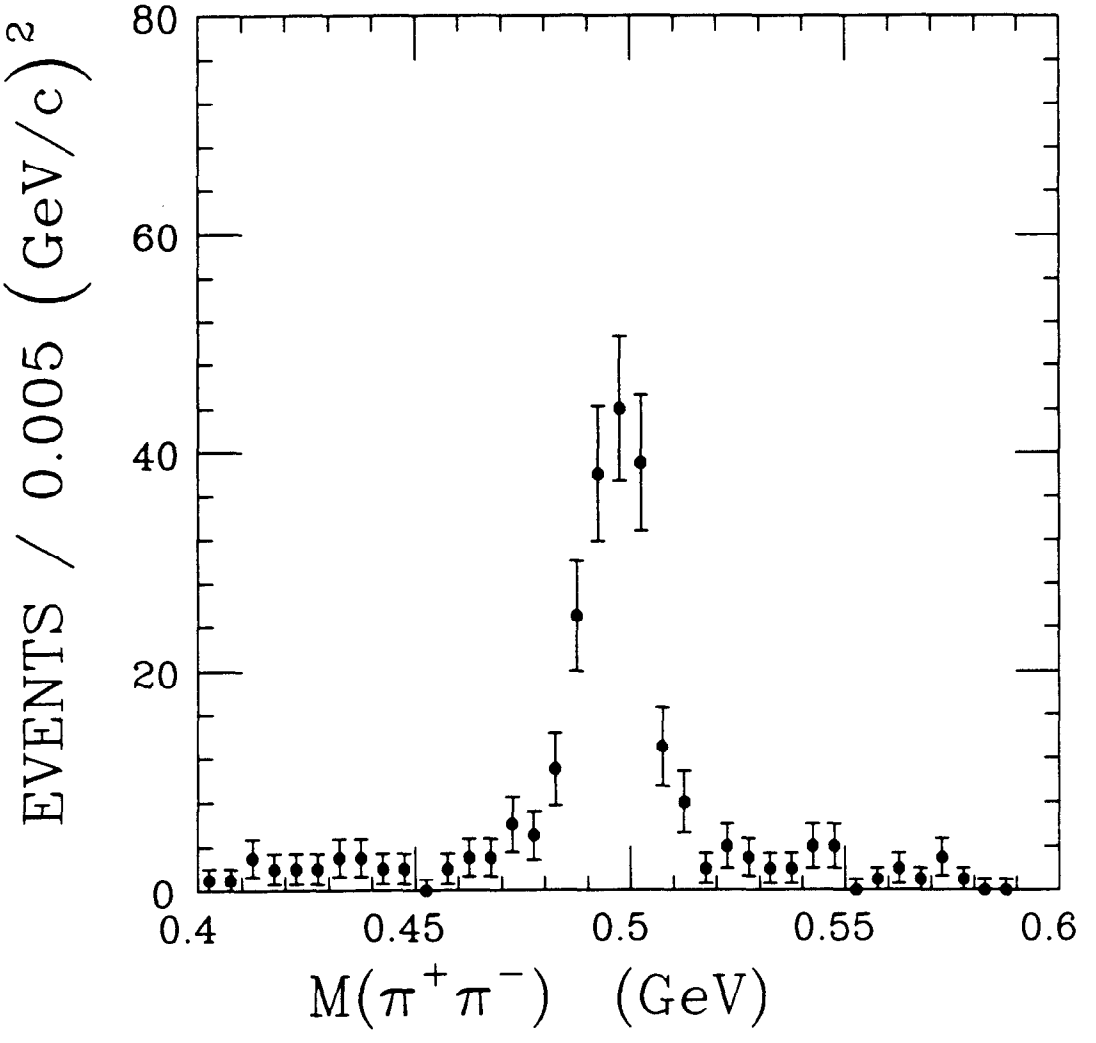
EVENTS / 0.005 (GeV/c)^2
80
60
40
20
0
0.4
0.45
0.5
0.55
0.6
M($\pi^+\pi^-$) (GeV)
XBL 874-1769

Figure 1

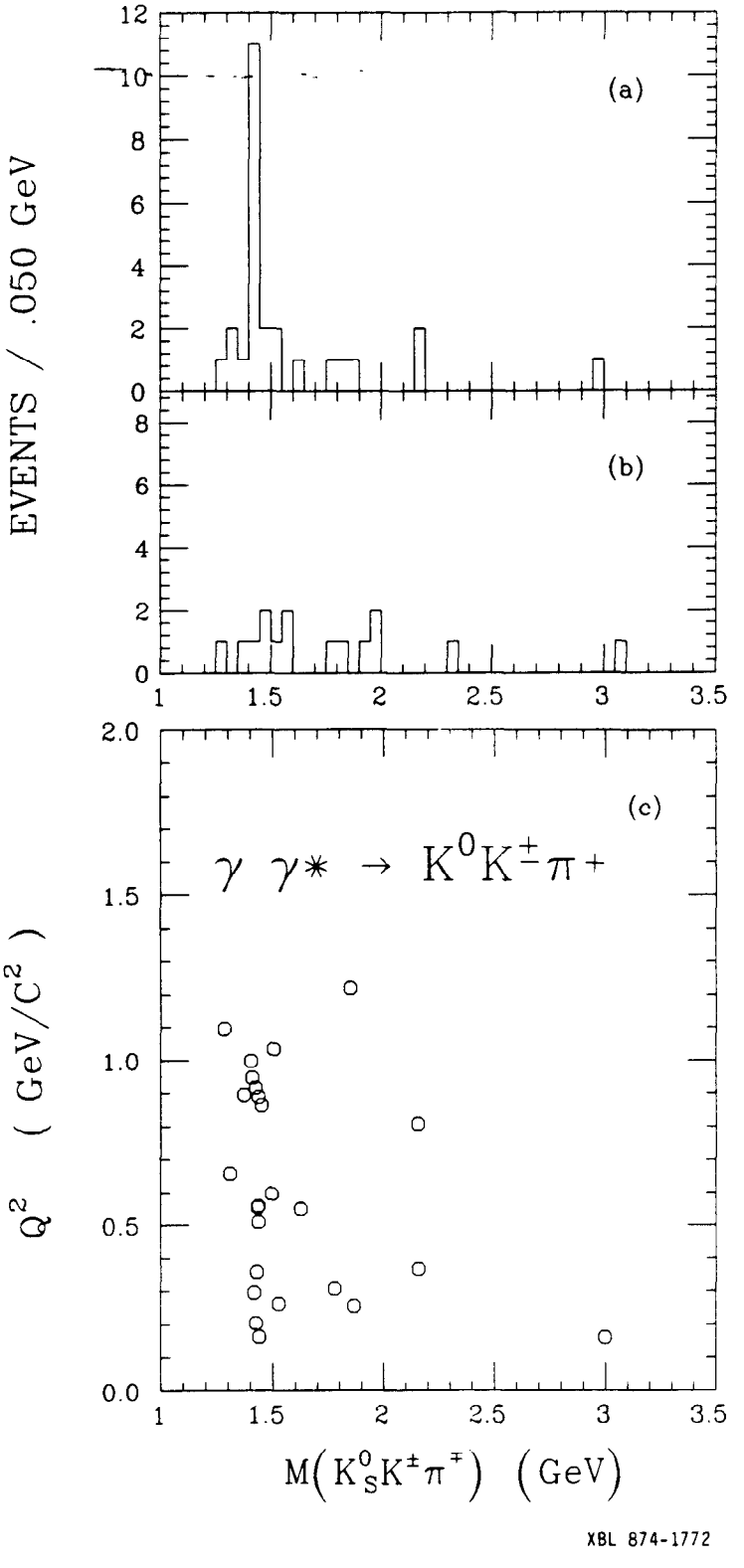
EVENTS / .050 GeV
(a)
(b)
(c)
$\gamma\ \gamma^* \rightarrow K^0K^{\pm}\pi^+$
Q^2 (GeV/C^2)
$M(K^0_S K^{\pm}\pi^{\mp})$ (GeV)
XBL 874-1772

Figure 2

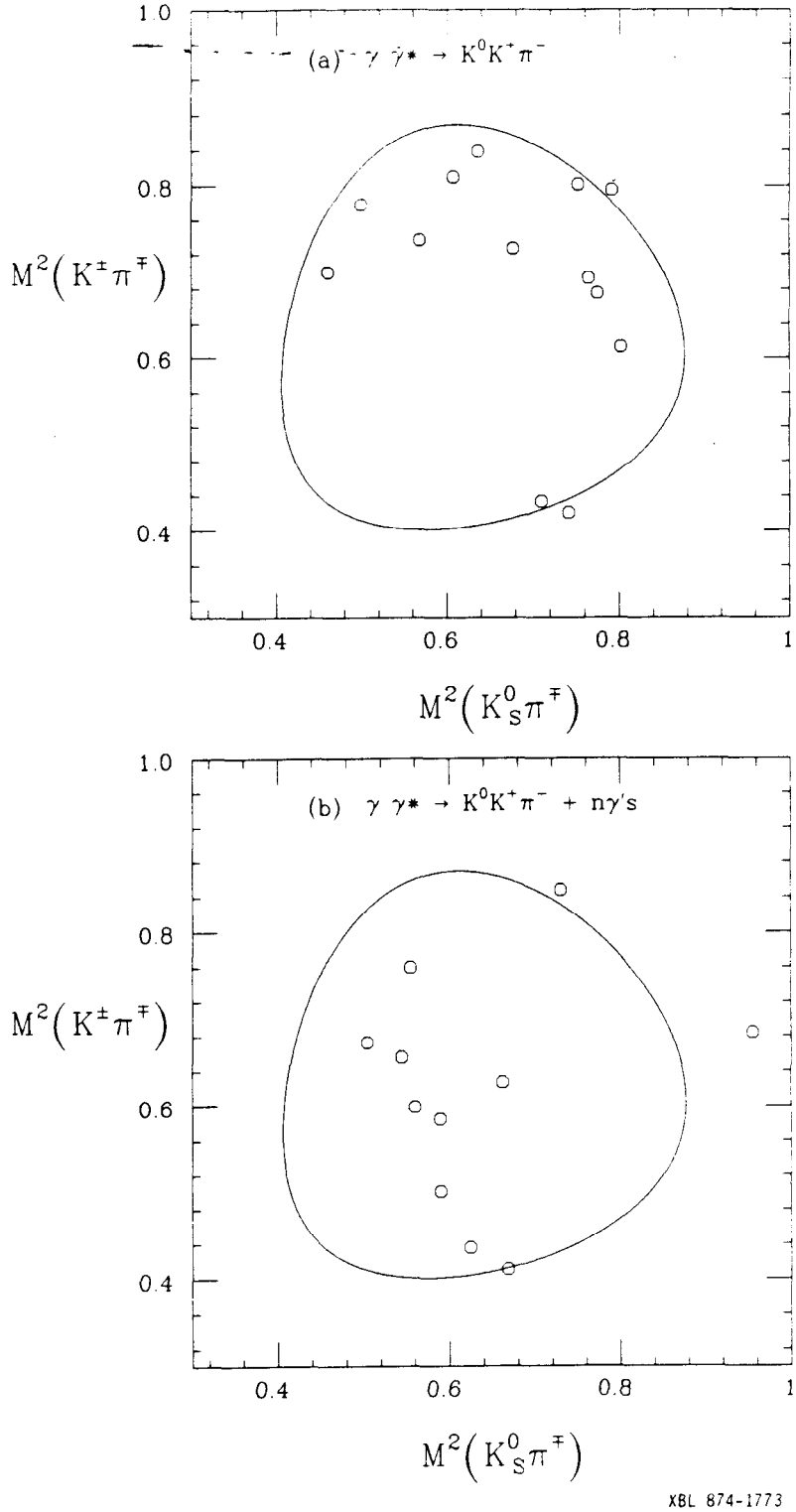
(a) $\gamma\,\gamma^* \to K^0K^+\pi^-$
(b) $\gamma\,\gamma^* \to K^0K^+\pi^- + n\gamma$'s
$M^2(K^\pm\pi^\mp)$
$M^2(K^0_S\pi^\mp)$
1.0
0.8
0.6
0.4
0.4
0.6
0.8
1
XBL 874-1773

Figure 3

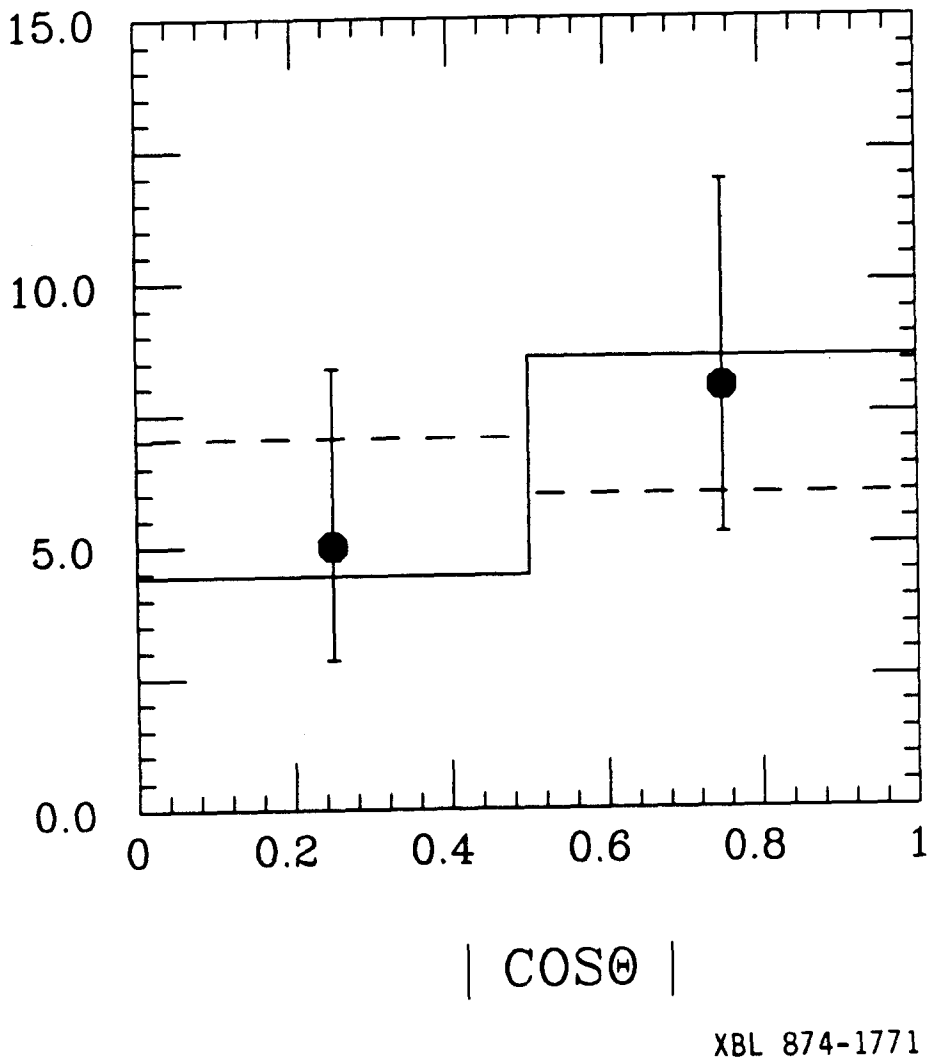

Figure 4